

See discussions, stats, and author profiles for this publication at: <https://www.researchgate.net/publication/230576822>

Kinetics and Mechanism of the Reaction between Thiosulfate and Chlorine Dioxide

ARTICLE in THE JOURNAL OF PHYSICAL CHEMISTRY A · SEPTEMBER 1998

Impact Factor: 2.69 · DOI: 10.1021/jp981714n

CITATIONS

26

READS

103

2 AUTHORS:



Attila K Horváth

University of Pécs

54 PUBLICATIONS 536 CITATIONS

SEE PROFILE



István Nagypál

University of Szeged

86 PUBLICATIONS 1,450 CITATIONS

SEE PROFILE

Kinetics and Mechanism of the Reaction between Thiosulfate and Chlorine Dioxide

Attila K. Horváth[†] and István Nagypál*

József Attila University, Institute of Physical Chemistry, Szeged, P.O. Box 105, H-6701, Hungary

Received: March 31, 1998; In Final Form: May 27, 1998

The reaction between thiosulfate and chlorine dioxide in slightly alkaline medium has been studied by stopped-flow techniques. The reaction cannot be studied under pseudo-first-order condition, thus a new approach based on the improved calibration and use of stopped-flow spectrophotometers was applied. The reaction starts with irreversible formation of $\cdot\text{S}_2\text{O}_3\text{ClO}_2^{2-}$ radical. The main path of the reaction produces tetrathionate and chlorite through the formation of light absorbing tetrathionate radical ($\cdot\text{S}_4\text{O}_6^{3-}$). Any of the reactant present in excess slightly modifies the 1:1 stoichiometry, and sulfate as well as chloride ions are also formed. A detailed mechanism based on a rigorous simultaneous fitting of the experimental data is proposed.

Introduction

Among the chlorite-driven chemical oscillators,¹ the thiosulfate–chlorite reaction gives some of the most exotic dynamics. The reaction is autocatalytic under batch condition,² and it exhibits oscillation in a CSTR.² A propagating reaction front may be generated in unstirred solutions³ and the reaction, in unbuffered solution, behaves as a clock reaction. The reaction time, however, varies irreproducibly within the first several minutes, even in identically prepared samples.⁴ Only the distribution of the reaction times is reproducible. A qualitative explanation of the irreproducibility is the parallel formation of SO_4^{2-} and $\text{S}_4\text{O}_6^{2-}$ ions accompanied by H^+ and OH^- formation with only a very slight increase of pH. The further reaction of $\text{S}_4\text{O}_6^{2-}$ with ClO_2^- is highly autocatalytic in H^+ . Thus, if the proton formation in a small part of the reactive solution overtakes the OH^- formation because of the local fluctuations, then it ignites the autocatalytic process and the reaction is over instantaneously. If the system avoids this in the first several minutes, then the OH^- concentration reaches a sufficient value to suppress any local fluctuations, and the system behaves as a regular clock reaction. The ultimate goal of the investigations of this system is to understand and describe quantitatively the wide range of “exotic” phenomena. For such a complex kinetic system, we have to investigate all the conceivable and accessible subsystems. As a part of the systematic kinetic studies on the subsystems, we have undertaken a detailed stoichiometric and kinetic study on the thiosulfate–chlorine dioxide reaction. The results of these investigations are presented in this paper. No kinetic studies on this system have been reported before. Preliminary stopped-flow experiments showed that the reaction could not be studied using the usual approach of pseudo-first-order conditions. The reaction is too fast in large thiosulfate excess and the change of the absorbance is too small if chlorine dioxide is in large excess. The only way of studying the reaction was by the application of comparable concentration of both reactants. The use of comparable concentrations posed many questions which led us to develop an improved calibration and use of stopped-flow instruments.⁵ The present paper is our first report of using the improved use of the stopped-flow method

in order to unravel the mechanism of an unknown reaction. It is also the first report of using ZiTa⁶ for numerically integrating the absorbance profile along the observation cell.⁵

Experimental Section

Materials. $\cdot\text{ClO}_2$ stock solution was prepared⁷ by oxidizing NaClO_2 solution in 10% H_2SO_4 by $\text{K}_2\text{S}_2\text{O}_8$. The $\cdot\text{ClO}_2$ evolved was purged out with an air stream and dissolved in cold water. The stock solution was kept refrigerated and protected from light. The stock solution was checked daily for Cl^- , H^+ , ClO_2^- , and ClO_3^- impurities after purging out its $\cdot\text{ClO}_2$ content. None of these impurities could be detected up to 1 month. The commercially available (Aldrich) NaClO_2 was purified as described.⁷ All other chemicals were the highest quality commercially available. All solutions were prepared with Milli-Q water, with $18.2 \mu\text{S cm}^{-1}$ conductivity. The ionic strength was adjusted to 0.5 M by NaClO_4 in all measurements, except for the ion chromatographic studies. The pH of the solutions was regulated between 7.5 and 9.5 by a boric acid–sodium hydroxide buffer.

Methods. The stoichiometry of the reaction was studied spectrophotometrically by measuring the spectra of the products up to 10 min after mixing the reactants directly in a 10 mm quartz cuvette equipped with Teflon cap. The chlorine dioxide stock solution was introduced directly into the cuvette from a fast delivery pipet as the last component, just before the cuvette was closed. The spectra of the solutions of the products were detected by Zeiss S10 diode array spectrophotometer between 266 and 450 nm up to 10 min in every minute. No detectable change in the spectra was detected after 1 min. The expected absorbing species in the product solution were the reagent in excess, as well as $\text{S}_4\text{O}_6^{2-}$ and ClO_2^- . (Cl^- and SO_4^{2-} do not absorb light in the given range.) We have determined the molar absorbance of these species prior to stoichiometric measurements. In separate series of experiments we checked if a linear algebraic decomposition of their composite spectra is an appropriate tool for precise analytical determination of their concentration. Figure 1 shows the molar absorbance of the species in question calculated from the spectrum of at least five solutions with different concentrations.

No change in the spectra of the prepared mixtures of $\text{S}_2\text{O}_3^{2-}$, $\text{S}_4\text{O}_6^{2-}$, and ClO_2^- in the given pH range was observed for 20

[†] E-mail: horvatha@chem.u-szeged.hu.

* To whom all correspondence should be addressed. E-mail: nagypal@chem.u-szeged.hu.

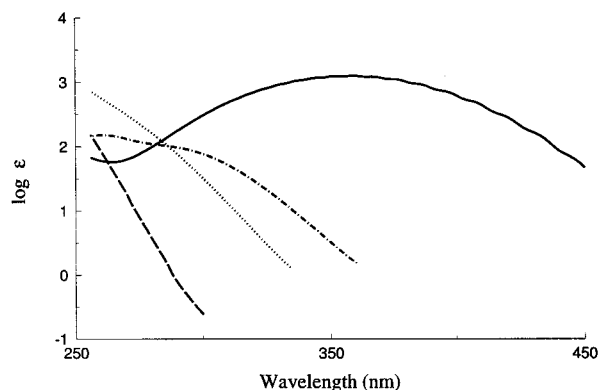


Figure 1. Molar absorbances of thiosulfate (long dashed line), tetrathionate (dots), and chlorite (dot-dashed line) ions and chlorine dioxide (solid line).

min. A systematic study of the linear algebraic decomposition of the spectra of many mixtures with known concentration showed that the accuracy of concentration determination for chlorite and tetrathionate ions is within 1% and for thiosulfate is within 8%. The reason for the inaccuracy of thiosulfate concentration is its low molar absorbance compared to the other two ions (see: Figure 1). To check the result of the stoichiometry established from the photometric experiments, several solutions of the products were analyzed by a WATERS Ionchromatograph. Kinetic measurements were carried on a Hi-Tech SF-61 stopped-flow instrument attached to M300 monochromator. Most of the runs were followed at 360 nm, where chlorine dioxide has its absorption maximum. In some cases (see below) the reaction was followed at four additional wavelengths (350, 380, 400, and 420 nm).

Data Treatment. Only the experimental data measured up to an absorption maximum of 1.4 have been used for the evaluation of the kinetic runs. Because all the kinetic curves contained 512 data points, the number of points in each run was reduced to about 100 to avoid unnecessary and time-consuming calculations. The point reduction was based on the principle of equivalent arclength in order to avoid losing any important chemical information. The next step of the evaluation was to carry out the matrix rank analysis on the absorbance-time data series to determine the number of absorbing species. The experimental curves were analyzed with the program package ZiTa,⁶ developed recently for fitting kinetic data. Altogether, 12 852 experimental points of the 131 absorbance-time series data points were used for simultaneous fitting. The sum of squares of the deviation between the experimentally measured and calculated absorbances was selected as a parameter to be minimized.

Results

Stoichiometric Studies. Ionchromatographic analysis was used to identify the sulfur-containing products formed in excess thiosulfate. The ionchromatographic column available under our condition (slightly alkaline pH) and for our possible products (sulfate, tetrathionate, polythionates, and excess thiosulfate) was Polyspher IC AN-1. The chlorine and sulfur-containing products cannot be determined simultaneously because of the huge difference in their retention times. Moreover, the chlorine-containing products can only be eluted in measurable retention time by acidic eluent on the given column, thus the further oxidation of tetrathionate and thiosulfate by chlorite^{4,8} would falsify the results. Therefore the eluent was chosen to be 2.5 mM parahydroxybenzoic acid dissolved in 10 volume-percentage methanol-water mixture. The pH of the eluent was

TABLE 1: The Initial $[S_2O_3^{2-}]_0$, $[^*ClO_2]_0$ and the Spectrophotometrically Determined $[S_4O_6^{2-}]_\infty$ as Well as $[ClO_2^-]_\infty$ Concentrations in Excess Thiosulfate. $SR = ([S_2O_3^{2-}]_0 - [S_2O_3^{2-}]_\infty)/[^*ClO_2]_0$

run	$[S_2O_3^{2-}]_0$ (mM)	$[^*ClO_2]_0$ (mM)	$[S_4O_6^{2-}]_\infty$ (mM)	$[ClO_2^-]_\infty$ (mM)	$\frac{[S_4O_6^{2-}]_\infty}{[ClO_2^-]_\infty}$	SR
1	6.06	2.21	0.870	1.360	0.640	1.006
2	6.67	2.41	0.964	1.470	0.656	1.020
3	7.75	2.24	0.910	1.370	0.664	1.030
4	8.76	2.22	0.902	1.350	0.668	1.032
5	9.70	2.17	0.881	1.310	0.673	1.034
6	3.49	1.67	0.681	0.980	0.694	1.045
7	3.97	1.61	0.665	0.915	0.727	1.064
8	4.42	1.56	0.647	0.881	0.734	1.068

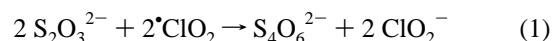
TABLE 2: The Initial $[S_2O_3^{2-}]_0$, $[^*ClO_2]_0$ and the Spectrophotometrically Determined $[ClO_2^-]_\infty$ Concentrations in Excess Chlorine Dioxide. $SR = ([S_2O_3^{2-}]_0)/([^*ClO_2]_0 - [^*ClO_2]_\infty)$

run	$[S_2O_3^{2-}]_0$ (mM)	$[^*ClO_2]_0$ (mM)	$[^*ClO_2]_\infty$ (mM)	SR
1	1.291	2.475	1.056	0.910
2	1.906	2.492	0.502	0.958
3	1.380	2.658	1.244	0.976
4	2.035	2.595	0.535	0.988
5	0.968	1.374	0.335	0.932
6	0.822	3.021	2.150	0.944
7	1.112	2.127	0.976	0.966

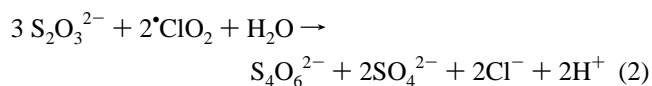
adjusted to 9.7 by *N,N*-diethylethanolamine. Besides the thiosulfate in excess, only tetrathionate could be detected. The quantitative evaluation of a large series of ionchromatographic measurements was in complete agreement with the results of the spectrophotometric studies (see below), therefore they are not given in detail. Table 1 summarizes the results of the photometric analysis of the products in excess thiosulfate.

In excess *ClO_2 , the unreacted *ClO_2 was determined from that range of the spectra where *ClO_2 is the only absorbing species. Table 2 summarizes the results.

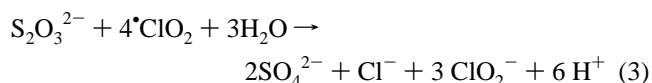
The data in Table 1 and 2 convincingly show that the basic stoichiometry is 1:1, i.e.,



but this stoichiometry is slightly shifted toward the reactant in excess. The photometric and ionchromatographic analysis of the products showed that only tetrathionate and sulfate, as well as chlorite and chloride ions, are formed in both conditions. Since no other sulfur- and chlorine-containing oxyanion could be detected, these observations imply that the stoichiometry is



in excess thiosulfate and that the stoichiometry



in excess chlorine dioxide should also be considered; and an appropriate linear combination of the three reactions may explain the results.

The most important characteristics of the kinetic curves. (1) In excess chlorine dioxide the reaction is completed within a few seconds as demonstrated in Figures 2 and 3. The preliminary data fitting showed that all the experimental curves can be fitted, in chlorine dioxide excess, as a sum of a second

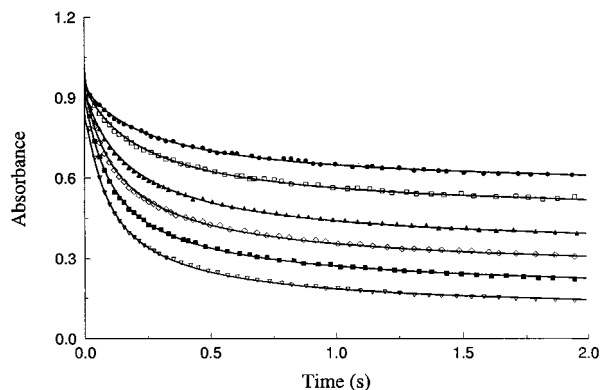


Figure 2. Experimental curves (symbols) in excess of chlorine dioxide. $[\text{ClO}_2]_0 \approx 9.3 \times 10^{-4} \text{ M}$, $\text{pH} = 8.55$; $[\text{S}_2\text{O}_3^{2-}]_0 \times 10^4 \text{ M} = 2.90$ (●), 3.77 (□), 4.84 (▲), 5.77 (◇), 6.44 (■), 6.88 (▽). Calculated curves are illustrated by solid line.

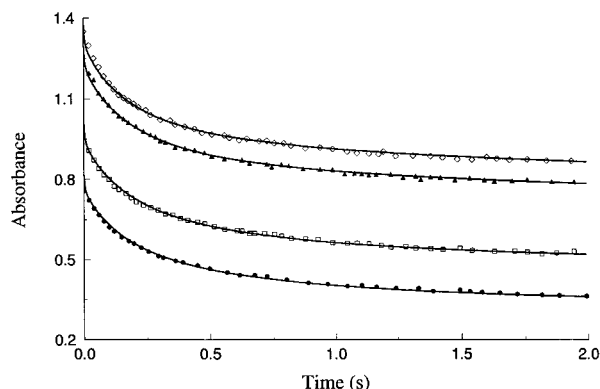


Figure 3. Experimental curves (symbols) in excess of chlorine dioxide. $[\text{S}_2\text{O}_3^{2-}]_0 = 3.70 \times 10^{-4} \text{ M}$, $\text{pH} = 8.55$; $[\text{ClO}_2]_0 \times 10^4 \text{ M} = 7.59$ (●), 9.34 (□), 11.9 (▲), 12.6 (◇). Calculated curves are illustrated by solid line.

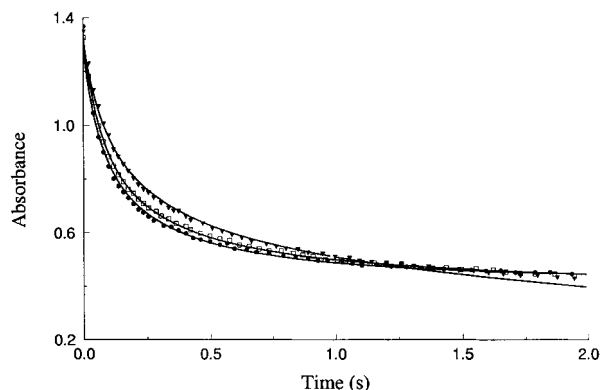


Figure 4. Experimental curves (symbols) in excess of chlorine dioxide. $[\text{S}_2\text{O}_3^{2-}]_0 = 7.9 \times 10^{-4} \text{ M}$, $[\text{ClO}_2]_0 \approx 1.3 \times 10^{-3} \text{ M}$, $\text{pH} = 7.58$ (●), 8.55 (□), 9.31 (▼). Calculated curves are illustrated by solid line.

and third-order rate law (both of them first order with respect to chlorine dioxide, first and second order with respect to thiosulfate). (2) Figure 4 shows that the reaction in chlorine dioxide excess is slightly dependent on pH. However, no pH-dependence was observed in excess thiosulfate, as depicted in Figure 5. (3) The sigmoidal-shaped kinetic curves are the most important feature in kinetic data in excess thiosulfate (Figures 6 and 7). Moreover, the increase thiosulfate by 1 order of magnitude decreases dramatically the reaction time by almost 2 orders of magnitude.

Matrix Rank Analysis (MRA). Matrix rank analysis^{9–12} was carried out, and the residual absorbance curves¹³ were calculated

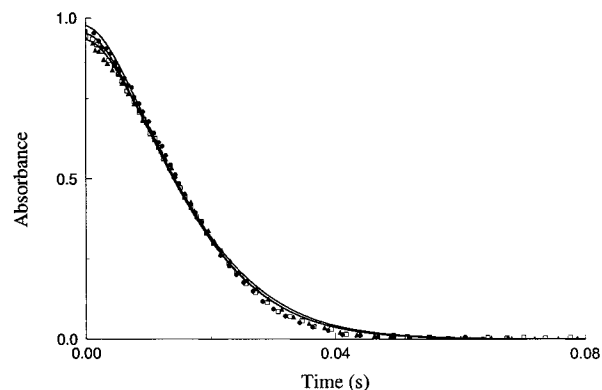


Figure 5. Experimental curves (symbols) in excess of thiosulfate. $[\text{S}_2\text{O}_3^{2-}]_0 = 1.95 \times 10^{-3} \text{ M}$, $[\text{ClO}_2]_0 \approx 9.7 \times 10^{-4} \text{ M}$, $\text{pH} = 7.48$ (●), 8.60 (□), 9.27 (▲). Calculated curves are illustrated by solid line.

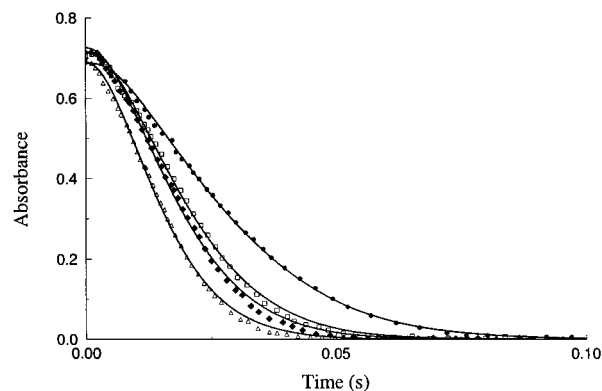


Figure 6. Experimental curves (symbols) in excess of thiosulfate. $[\text{ClO}_2]_0 \approx 7.2 \times 10^{-4} \text{ M}$, $\text{pH} = 9.27$; $[\text{S}_2\text{O}_3^{2-}]_0 \times 10^3 \text{ M} = 1.28$ (●), 1.51 (□), 1.59 (◆), 1.71 (△). Calculated curves are illustrated by solid line.

on the sets of experimental data measured at five different wavelengths. The rank of the matrixes was found to be 2 in both excesses. It follows that a species absorbing light in the 350–420 wavelength range is formed during the reaction. The residual absorbance–time curve, visual illustration of matrix rank analysis, is a deciding evidence of the presence of an absorbing intermediate, as can be seen in Figure 8. Dogliotti and Hayon¹⁴ reported the flash photolysis study, while Schönešhöfer¹⁵ the pulse radiolysis of thiosulfate solution. It was found in these works that radiation of thiosulfate solution yielded a relatively long-lived, with a lifetime of some milliseconds, transient species with a strong absorbance band in the 340–440 nm wavelength range. The maximum of this band was between 370–380 nm with a $1650\text{--}1720 \text{ M}^{-1}\text{cm}^{-1}$ molar absorbance.^{14,15} Essential difference in the interpretation of the results is that Dogliotti and Hayon identified this transient as thiosulfate radical, while Schönešhöfer as tetrathionate radical. The results of kinetic measurements in Schönešhöfer's paper showed that the thiosulfate radical was yielded by a first, rapid step of irradiation, followed the thiosulfate radical reacting further with thiosulfate ion to result in a tetrathionate radical. These results are generally accepted,¹⁶ thus it seems to be logical to assume that tetrathionate radical is the second absorbing intermediate species in the thiosulfate–chlorine dioxide system. Another important result of Schönešhöfer's work is that the thiosulfate ion catalyzes the decomposition of tetrathionate radical. The catalytic effect will be analyzed and compared to our results later.

Proposed Mechanism. The mechanism proposed is based on a rigorous simultaneous fitting of 131 experimental curves. The

TABLE 3: Initial Concentrations and Concentration Ranges of the Reactants in the Kinetic Experiments Given in mM dm⁻³ Unit

[*ClO ₂] ₀	[S ₂ O ₃ ²⁻] ₀	pH	runs
0.33–1.35	0.211–0.908	7.58	21
0.50–1.22	1.32–1.97	7.48	17
0.38–1.34	0.215–1.09	8.55	31
0.55–1.18	1.28–1.98	8.60	14
0.42–1.34	0.191–1.06	9.31	32
0.50–1.17	1.21–1.89	9.27	17

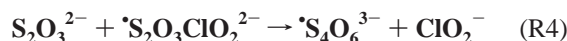
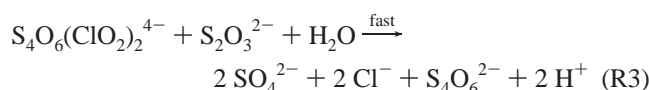
concentration ranges of the reactants in the samples are collected in Table 3. Several hundred models have been used to try quantitatively describe the experimental curves. Some of the trials will be dealt with in the discussion. The following reaction mechanism was suggested, which is in qualitative and quantitative agreement with all experiments:



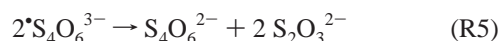
$$v_1 = k_1[\bullet\text{ClO}_2][\text{S}_2\text{O}_3^{2-}]$$



$$v_2 = k_2[\bullet\text{S}_2\text{O}_3\text{ClO}_2^{2-}]^2$$



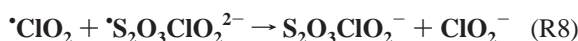
$$v_4 = k_4[\text{S}_2\text{O}_3^{2-}][\bullet\text{S}_2\text{O}_3\text{ClO}_2^{2-}]$$



$$v_5 = k_5[\bullet\text{S}_4\text{O}_6^{3-}]^2$$

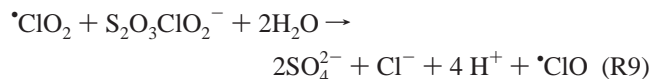


$$v_6 = k_6[\bullet\text{S}_4\text{O}_6^{3-}][\text{S}_2\text{O}_3^{2-}]$$

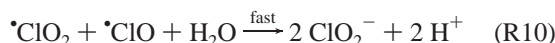


$$v_{8a} = k_{8a}[\bullet\text{ClO}_2][\bullet\text{S}_2\text{O}_3\text{ClO}_2^{2-}]$$

$$v_{8b} = k_{8b}[\bullet\text{ClO}_2][\bullet\text{S}_2\text{O}_3\text{ClO}_2^{2-}][\text{OH}^-]$$



$$v_9 = k_9[\text{S}_2\text{O}_3\text{ClO}_2^-][\text{OH}^-][\bullet\text{ClO}_2]$$



Discussion

The crucial steps in the proposed mechanism are emphasized by bold face printing. The initial step R1 is an irreversible association of the reactants yielding $\bullet\text{S}_2\text{O}_3\text{ClO}_2^{2-}$ radical. The inclusion of the reverse reaction of (R1) into the model decreases

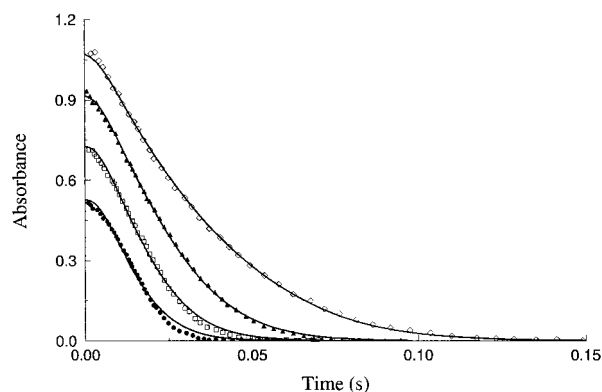


Figure 7. Experimental curves (symbols) in excess of thiosulfate. $[\text{S}_2\text{O}_3^{2-}]_0 = 1.55 \times 10^{-3}$ M, pH = 9.27; $[\bullet\text{ClO}_2]_0 \times 10^4$ M = 5.34 (●), 7.39 (□), 9.35 (▲), 11.0 (◇). Calculated curves are illustrated by solid line.

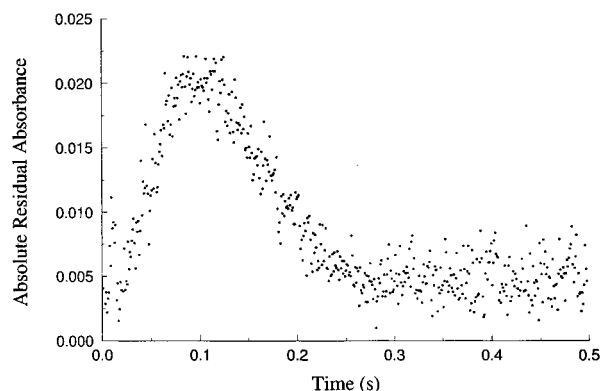
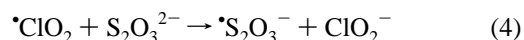
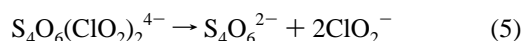


Figure 8. The residual absorbance¹³ as a function of time in case of pH = 8.51, $[\text{S}_2\text{O}_3^{2-}]_0 = 1.02 \times 10^{-3}$ M, $[\bullet\text{ClO}_2]_0 = 5.38 \times 10^{-4}$ M.

the average absorbance deviation with less than 2% (i.e., it is not justified by the calculations). Any attempt to replace step R1 with either reversible or irreversible initial step of a possible



reaction failed. We have also tried to assign absorbance to $\bullet\text{S}_2\text{O}_3\text{ClO}_2^{2-}$, but the average deviation only slightly decreased and the molar absorption coefficient calculated was less than $100 \text{ M}^{-1} \text{ cm}^{-1}$. Therefore, this radical was considered in the final calculations as a nonabsorbing species at 360 nm. The high rate constant calculated for the first step means that the reactant, which is not in excess, practically disappears from the solution within 100 ms and that the further change (see Figures 2–4) is determined by the proceeding steps between the intermediates and the reactant in excess. The $\bullet\text{S}_2\text{O}_3\text{ClO}_2^{2-}$ formed in the first step has three paths for the further transformation. Step R2 is its dimerization followed by a fast step R3. (The fast steps R3, R7, and R10 were taken into account with fixed rate constants of $10^9 \text{ M}^{-1} \text{ s}^{-1}$.) Steps R1–R3 together lead to the stoichiometry given by eq 2 (i.e., to the stoichiometry which is responsible for the slight deviation of 1:1 stoichiometric ratio in thiosulfate excess (Table 1)). Any trial to replace step R3 by the reaction 5



or to add to it the final model failed. Neither rate coefficient for eq 5 nor its ratio to k_3 could be calculated. If steps R2 and R3 are omitted from the proposed mechanism, then the average deviation of the best fit increases to 0.0250 absorbance unit.

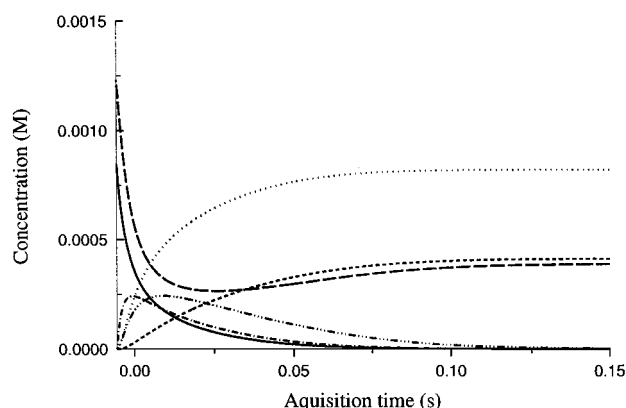
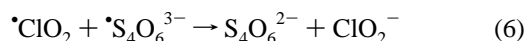


Figure 9. Concentration of the species as a function of time in excess thiosulfate [ClO_2] $_0 = 8.45 \times 10^{-4}$ M, pH = 9.27, [$\text{S}_2\text{O}_3^{2-}$] $_0 = 1.23 \times 10^{-3}$ M. ClO_2 (solid line), $\text{S}_2\text{O}_3^{2-}$ (long dashed line), $\text{S}_2\text{O}_3\text{ClO}_2^{2-}$ (dot dashed line), $\text{S}_4\text{O}_6^{2-}$ (dot-dot dashed line), $\text{S}_4\text{O}_6^{2-}$ (short dashed line), ClO_2^- (dots). Note that the acquisition starts at $t = 0$. The concentrations between $-t_s$ and 0 are calculated by integration back from the measured range.⁵

The main path in thiosulfate excess starts with step R4, producing tetrathionate radical. Its calculated molar absorbance of $2115 \text{ M}^{-1} \text{ cm}^{-1}$ at 360 nm is in good agreement with Schöneshöfer's data, who obtained a value of $1650 \text{ M}^{-1} \text{ cm}^{-1}$ at 370 nm based on pulse radiolysis experiments. Its decomposition proceeds through the rate determining steps R5 and R6. In step R5 the recombination of the absorbing tetrathionate radical takes place and the reactant thiosulfate is formed back. Step R6 is a catalytic process with respect to thiosulfate ion forming thiosulfate radical which disappears rapidly in step R7. The stoichiometry of step R5 as well as of steps R6 and R7 are the same, but steps R6 and R7 have a significant role only in thiosulfate excess. Steps R5 and R6 with R7 are responsible for the increase of the thiosulfate ion concentration in the final stage of the reaction, which is illustrated in Figure 9.

This overshoot–undershoot behavior¹⁷ frequently occurs in exotic reaction systems. It should be mentioned that the catalytic decomposition of the tetrathionate radical was earlier suggested by Schöneshöfer,¹⁵ but the specified products according to his work were hexathionate and sulfite ions. Our ionchromatographic results indicated that these ions are not formed in detectable amount under our experimental conditions. It is interesting that our suggested k_6 agrees perfectly with the value of $7.3 \times 10^4 \text{ M}^{-1} \text{ s}^{-1}$ determined by Schöneshöfer for the same reaction. Another consequence of the catalytic effect of thiosulfate is that the lifetime of tetrathionate radical is much longer in chlorine dioxide than in excess thiosulfate. Therefore the following reaction



seemed to be plausible in excess chlorine dioxide. Its rate coefficient was found to be about $1300 \text{ M}^{-1} \text{ s}^{-1}$. Because the average deviation of the data decreased by less than 3% and the standard error of this parameter was found to be too large compared to the others, this process was not proposed in the final model. If the main path (steps R4–R7) was omitted from the model the average absorbance deviation increased dramatically from 0.0089 to 0.0605. If either step R5 or step R6 (with R7) was omitted then the average deviation also increased significantly in both cases from 0.0089 to 0.0350 and 0.0432, respectively. For the sake of completeness, the molar absorbance of tetrathionate radical was also omitted from the model, and 0.0400 average absorbance deviation was found. Step R8 is the third path of the reaction of the $\cdot\text{S}_2\text{O}_3\text{ClO}_2^{2-}$ radical with chlorine dioxide to form in pH-independent (k_{8a}) and pH-dependent (k_{8b}) processes a nonabsorbing species $\text{S}_2\text{O}_3\text{ClO}_2^-$ analogous to the intermediate $\text{S}_2\text{O}_3\text{ClO}^-$ proposed in the chlorite–thiosulfate system.⁴ This path is responsible for the slight deviation of the stoichiometric ratio from 1:1 in chlorine dioxide excess. It is followed by a rate-determining pH-dependent step R9 and a fast reaction R10. Steps R8–R10 are responsible for the slight pH-dependence in chlorine dioxide excess and gives back the stoichiometry (eq 3). If the whole path is omitted from the model, a significant increase (0.0530) can be experienced in the average absorbance deviation. Omitting either the k_{8a} or the k_{8b} from the model leads to the average absorbance deviation 0.0580 and 0.0121, respectively. A new way of calculation to evaluate the data provided by the stopped-flow instrument has been suggested recently.⁵ The calculation requires the filling time of the observation cell (t_f) and the hypothetical starting time (t_s). The filling time was determined physically as described.⁵ t_s was fitted together with the parameters of the proposed model. The hypothetical starting time of the reaction was found to be in good agreement with the results obtained in different chemical systems^{5,18} investigated by our stopped-flow instrument. Omitting both the hypothetical starting time and filling time from the final model leads to a 0.0107 average absorbance deviation. The calculated rate constants, the molar absorbance of the tetrathionate radical, and their standard deviations are shown in Table 4.

The average deviation between the measured and calculated absorbances using all the 10 fitted (8 rate coefficients, 1 molar absorbance, and the hypothetical starting time⁵) and 4 fixed parameters (the filling time of the observation cell, k_3 , k_8 , and k_{10}) on the whole 131 absorbance–time series data points was found to be 0.0089 absorbance unit, which is close to the experimentally achievable limit of error with our stopped-flow spectrophotometer. The filling time was determined independently in an earlier work,⁵ therefore it was fixed to be 0.0039 s during the calculations. Typical results are illustrated in Figures 2–7.

TABLE 4: Rate Constants Calculated by the Different Fitting Methods and the Suggested Results with Their Standard Deviations

	absolute fit	relative fit	orthogonal fit	suggested value
$k_1 \times 10^{-5} (\text{M}^{-1} \text{ s}^{-1})$	1.82 ± 0.01	1.83 ± 0.01	1.67 ± 0.02	1.8 ± 0.1
$k_2 \times 10^{-3} (\text{M}^{-1} \text{ s}^{-1})$	7.21 ± 0.10	6.72 ± 0.07	6.82 ± 0.07	6.9 ± 0.3
$k_4 \times 10^{-5} (\text{M}^{-1} \text{ s}^{-1})$	2.80 ± 0.03	2.76 ± 0.03	2.62 ± 0.04	2.7 ± 0.1
$k_5 \times 10^{-4} (\text{M}^{-1} \text{ s}^{-1})$	4.37 ± 0.02	4.73 ± 0.03	5.07 ± 0.03	4.7 ± 0.4
$k_6 \times 10^{-4} (\text{M}^{-1} \text{ s}^{-1})$	7.18 ± 0.05	7.26 ± 0.06	7.56 ± 0.08	7.3 ± 0.2
$k_{8a} \times 10^{-3} (\text{M}^{-1} \text{ s}^{-1})$	5.45 ± 0.05	5.10 ± 0.04	5.12 ± 0.04	5.2 ± 0.2
$k_{8b} \times 10^{-8} (\text{M}^{-2} \text{ s}^{-1})$	1.12 ± 0.01	1.00 ± 0.01	1.13 ± 0.01	1.1 ± 0.1
$k_9 \times 10^{-7} (\text{M}^{-2} \text{ s}^{-1})$	1.99 ± 0.02	2.11 ± 0.01	2.03 ± 0.01	2.0 ± 0.1
$\epsilon_{\text{tetr.rad.}} (\text{M}^{-1} \text{ cm}^{-1})$	2115 ± 14	2130 ± 17	2326 ± 22	
$t_s \times 10^{-3} (\text{s})$	-5.60 ± 0.04	-5.42 ± 0.05	-6.53 ± 0.08	

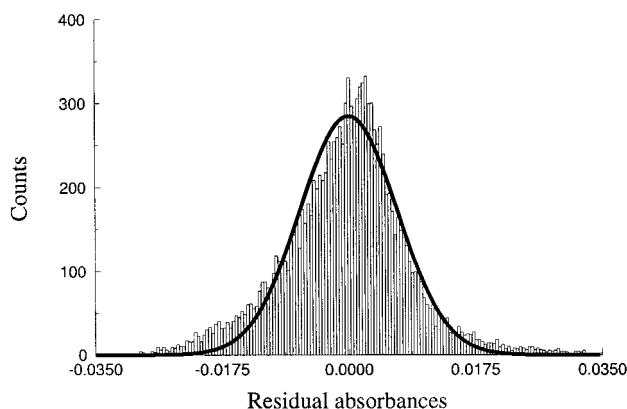


Figure 10. Histogram of the residual absorbances.

Figure 10 illustrates the histogram constructed from the deviations of all the points together with the best fitting error function. The almost regular distribution of the deviations convincingly shows that the model error cannot be significant. The standard errors of the parameters calculated by minimizing the sum of the squares of absolute deviations between the measured and calculated absorbances seem to be unrealistically small. To check the reliability of these data we also carried out relative and orthogonal fittings with the proposed model. Relative fitting means that the deviation between the measured and calculated data is normalized to the largest change of the absorbance in the given experiment and that the square-sum of these is minimized. Orthogonal fitting means that every experimental absorbance—time series is transformed into a $0 \leq x, y \leq 1$ “box” and that the square-sum of the perpendicular deviation in this box is minimized. The best fits were found to be 0.0159 and 0.0106 in the case of relative and orthogonal fittings, respectively. The agreement of the rate coefficients calculated by the three different minimization methods does not differ significantly, but the difference is out of the range of the standard errors. Therefore, the realistic values and standard errors given in the last column of Table 4 were calculated from the average of the three types of fitting.

Summary

The fast reaction between thiosulfate and chloride dioxide in slightly alkaline medium was studied by using the following three methods elaborated recently: (1) A multipurpose kinetic

program package, ZiTa,⁶ suitable for simultaneous evaluation of many curves characterized by the same kinetic model and parameter set; (2) the use of matrix rank analysis in order to determine the residual absorbances¹³ for the demonstration of the presence of an absorbing intermediate; and (3) an improved calibration and use of stopped-flow spectrophotometers based on the filling time and the hypothetical starting time.⁵ Combined application of the methods revealed that the reaction proceeds through three intermediates, namely, $\text{S}_2\text{O}_3\text{ClO}_2^{2-}$, $\text{S}_4\text{O}_6^{3-}$, and $\text{S}_2\text{O}_3\text{ClO}_2^-$. Among these, the tetrathionate radical has significant absorbance at 360 nm. A mechanism is proposed which describes 12 852 points in 131 different experimental curves with an average deviation of less than 0.010 absorbance unit.

Acknowledgment. The help of Gábor Ács in the ionchromatographic measurements, as well as the many helpful discussions with Gábor Peintler, is gratefully acknowledged. This work was supported by the National Science Foundation of Hungary (OTKA) (Grant T017257).

References and Notes

- (1) Rábai, Gy.; Orbán, M. *J. Phys. Chem.* **1993**, *97*, 5935.
- (2) Orbán, M.; De Kepper, P.; Epstein, I. R. *J. Phys. Chem.* **1982**, *86*, 431.
- (3) Nagypál, I.; Bazsa, Gy.; Epstein, I. R. *J. Am. Chem. Soc.* **1986**, *108*, 3635.
- (4) Nagypál, I.; Epstein, I. R. *J. Phys. Chem.* **1986**, *90*, 6285.
- (5) Peintler, G.; Horváth, A. K.; Nagy, A.; Nagypál, I. *J. Phys. Chem.* **1998**. Submitted for publication.
- (6) Peintler, G. *ZiTa, Version 4.2, a Comprehensive Program Package for Fitting Parameters of Chemical Reaction Mechanism*. Attila József University: Szeged, Hungary, 1989.
- (7) Peintler, G.; Nagypál, I.; Epstein, I. R. *J. Phys. Chem.* **1990**, *94*, 2954.
- (8) Peintler, G.; Nagypál, I.; Epstein, I. R. In *proceedings of the International Conference on Dynamics of Exotic Phenomena in Chemistry*; Hajdúszoboszló, Hungary, August 22–25, 1989; Abstract 237.
- (9) Ainsworth, S. *J. Phys. Chem.* **1961**, *65*, 1968.
- (10) Wallace, R. M.; Katz, S. M. *J. Phys. Chem.* **1964**, *68*, 3890.
- (11) Katakis, D. *Anal. Chem.* **1965**, *37*, 876.
- (12) Hugus, Z. Z.; El-Awady, A. A. *J. Phys. Chem.* **1971**, *75*, 2954.
- (13) Peintler, G.; Nagypál, I.; Jancsó, A.; Kustin K.; Epstein, I. R. *J. Phys. Chem. A* **1997**, *101*, 8013.
- (14) Dogliotti, L.; Hayon, E. *J. Phys. Chem.* **1968**, *72*, 1800.
- (15) Schöneshöfer, M. *Int. J. Radiat. Phys. Chem.* **1973**, *5*, 375.
- (16) Hug, G. L. *Optical Spectra of Nonmetallic Inorganic Transient Species in Aqueous Solution*, National Bureau of Standards, U.S. Department of Commerce: Washington, DC, 1981.
- (17) Rábai, Gy.; Bazsa, Gy.; Beck, M. T. *J. Am. Chem. Soc.* **1979**, *101*, 6746.
- (18) Nagy, A.; Peintler, G.; Nagypál, I. Unpublished results.